HHS Public Access

Author manuscript

DNA Repair (Amst). Author manuscript; available in PMC 2023 January 28.

Published in final edited form as:

DNA Repair (Amst). 2022 January ; 109: 103258. doi:10.1016/j.dnarep.2021.103258.

Incorporation of 5',8-cyclo-2'deoxyadenosines by DNA repair polymerases via base excision repair

Pawlos S. Tsegay[1], **Daniela Hernandez**[2], **Christopher Brache**[2], **Chryssostomos Chatgilialoglu**[3], **Marios G. Krokidis**[4], **Prem Chapagain**[5,6], **Yuan Liu**[1,2,6,*]

[1]Biochemistry Ph.D. Program, Florida International University, Miami, FL, USA

[2]Department of Chemistry and Biochemistry, Florida International University, Miami, FL, USA

[3]ISOF, Consiglio Nazionale delle Ricerche, Via P. Gobetti 101, 40129 Bologna, Italy;

[4]Institute of Nanoscience and Nanotechnology, N.C.S.R. "Demokritos," 15341, Agia Paraskevi, Athens, Greece.

[5]Department of Physics, Florida International University, Miami, FL, USA

[6]Biomolecular Sciences Institute, Florida International University, Miami, Florida, USA

Abstract

5',8-cyclo-2-deoxy nucleosides (cdPus) are the smallest tandem purine lesions including 5',8cyclo-2'-deoxyadenosine (cdA) and 5',8-cyclo-2'-deoxyguanosine (cdG). They can inhibit DNA and RNA polymerases causing mutations, DNA strand breaks, and termination of DNA replication and gene transcription. cdPus can be removed by nucleotide excision repair with low efficiency allowing them to accumulate in the genome. Recent studies suggest that cdPus can be induced in damaged nucleotide pools and incorporated into the genome by DNA polymerases. However, it remains unknown if and how DNA polymerases can incorporate cdPus. In this study, we examined the incorporation of cdAs by human DNA repair polymerases, DNA polymerases β (pol β), and pol η during base excision repair. We then determined the efficiency of cdA incorporation by the polymerases using steady-state kinetics. We found that pol β and pol η incorporated cdAs opposite dT and dC with low efficiency, and incorporated cdAs were readily extended and ligated into duplex DNA. Using molecular docking analysis, we found that the 5',8-covalent bond in cdA disrupted its hydrogen bonding with a template base suggesting that the phosphodiester bond between the 3'-terminus nucleotide and the α-phosphate of cdATP were generated in the absence of hydrogen bonding. The enzyme kinetics analysis further suggests that pol β and pol η increased their substrate binding to facilitate the enzyme catalysis for cdA incorporation. Our study reveals unique mechanisms underlying the accumulation of cdPu lesions in the genome resulting from nucleotide incorporation by repair DNA polymerases.

[*]Correspondence: yualiu@fiu.edu.

Conflict of interest

The authors declare no conflict of interest

Graphical Abstract

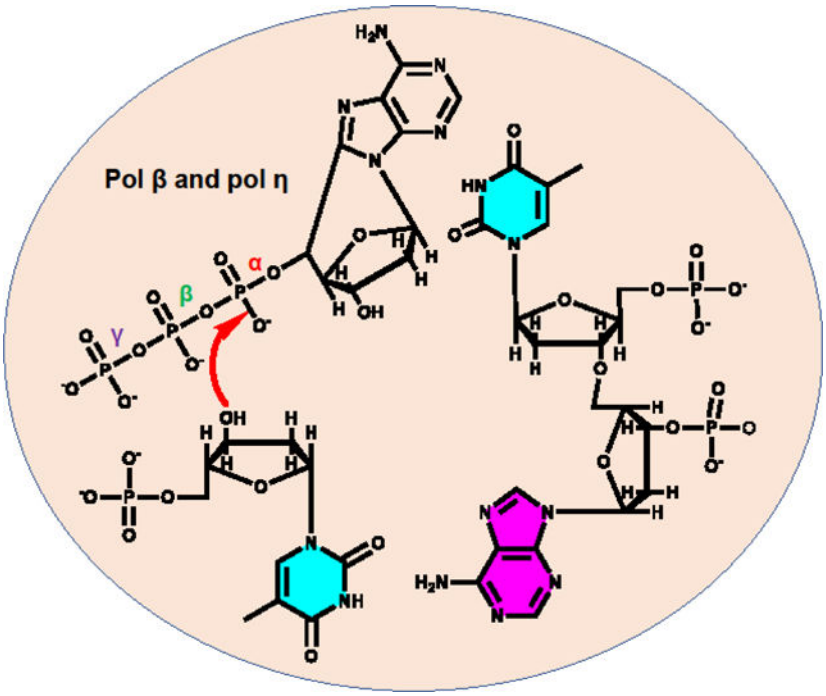

Keywords

5′,8-cyclo-2′-deoxyadenosine; DNA polymerase β; DNA polymerase η; incorporation of cyclo-deoxypurine lesions; base excision repair; steady-state kinetics of cyclo-deoxypurine incorporation

1. Introduction

The human genome is constantly damaged by endogenous and exogenous agents [1]. Among them, reactive oxygen species (ROS) are the most common form of DNA damaging agents that can result in various oxidized DNA base lesions [2, 3]. These include 5', 8-cyclo-2'-deoxyadenosine (cdA) and 5', 8- cyclo-2'-deoxyguanosine (cdG), which are referred to as 5', 8-cyclopurines (cdPus) [4–7]. cdA and cdG contain a covalent bond between C5' of the 2'-deoxyribose and C8 of adenine and guanine [6] that adopts 5'-R or 5'-S diastereoisomer. The additional covalent bond between the sugar backbone and base of cdPus can distort DNA structure [3, 8, 9] and prevent the base excision repair (BER) enzyme, DNA glycosylases, from removing the lesions [10, 11]. A significant amount of cdPu lesions are detected in the mammalian genome. The lesions are stable compared with other oxidatively generated DNA adducts and cannot be artificially produced during DNA isolation [4, 8, 12].

Unlike other oxidized DNA base lesions repaired by BER, cdPu lesions are repaired by nucleotide excision repair (NER) [10, 13, 14]. However, NER repairs cdPu lesions two to fourfold less efficiently than other types of bulky DNA adducts [13]. This results in the accumulation of the lesions in the genome leading to the inhibition of DNA and RNA

polymerase activities and DNA binding of transcription factors, replication fork stalling, and transcription termination [10, 14–17]. To overcome the challenges, cells have evolved a mechanism to bypass cdPu lesions through DNA repair, translesion DNA polymerases, and RNA polymerase II. The DNA repair polymerases that can bypass cdA lesions include DNA polymerase β (pol β), pol η, pol I, and pol ζ [18–23]. However, bypass cdPu lesions by DNA polymerases and RNA polymerases can also incorporate incorrect nucleotides or result in DNA and RNA synthesis stalling [18, 20, 21, 23–25]. Pol β stalls after incorporating a dT opposite cdA creating single-strand breaks [20]. On the other hand, RNA polymerase II and pol β can also cause multi-nucleotide deletion and repeat deletion to bypass cdAs during transcription and BER [19, 21]. Thus, the accumulation of cdPu lesions in the human genome can result in mutations and genome instability associated with pathological conditions, including aging, inflammation, carcinogenesis, and neurodegeneration [4, 5, 26–28].

Endogenous and exogenous ROS can damage DNA bases in the genome and the nucleotide pool [29, 30]. It is implicated that the nucleotide pool is more susceptible to ROS than the genomic DNA. Previous studies have shown that ROS induces more 8-oxoGTP and 2-hydroxy adenosine triphosphate than 8-oxoG and oxidized adenosine generated in the genomic DNA [29–31]. This further suggests a possibility that DNA polymerases may incorporate oxidized nucleotides triphosphate to create DNA damage during DNA replication and repair. It has been found that DNA polymerases incorporate an 8-oxoG to basepair with A and C efficiently [32]. The incorporated damaged nucleotide can be further extended, allowing the damaged base to be integrated into the genomic DNA [32, 33]. The findings indicate that DNA polymerases can compromise genome integrity by incorporating incorrect and/or damaged nucleotides such as 8oxoG from the damaged nucleotide pool. Since cdPus can also be generated in the nucleotide pool, we hypothesized that human DNA polymerases can incorporate cdPu triphosphate into DNA during DNA repair. To test our hypothesis, we examined the incorporation of cdA triphosphate by human repair DNA polymerases during BER and determined the catalytic efficiency of cdA incorporation using steady-state kinetics. For the first time, we found that human repair DNA polymerases incorporated cdATP into duplex DNA. We showed that pol β and translesion DNA polymerase, pol η, incorporated both 5’-RcdA and 5’-ScdA to basepair with dT. However, both polymerases also misincorporated cdA to basepair with dC more efficiently than with dT, suggesting that the incorporation of cdAs by repair DNA polymerases can introduce cdPu lesions in genomic DNA while it preferentially causes mutations. Using molecular docking analysis, we demonstrated that in the active sites of pol β and pol η, cdA exhibited a distorted configuration that disrupted its hydrogen bonding with template bases. The results suggest that the phosphodiester bond between cdA and the 3’-terminus nucleotide of the primer was created by the nucleophilic attack from the 3’-hydroxy group to the α-phosphate of cdATP in the absence of the hydrogen bonds. The enzyme kinetics analysis suggests that the repair DNA polymerases managed to increase the catalysis for cdA incorporation by improving their substrate binding. The results further revealed the structural and functional basis underlying the incorporation of cdA by repair DNA polymerases and the mutagenic effects resulting from cdA incorporation.

2. Materials and methods

2.1 Materials

5′*R*- and 5′*S*-diastereoisomers of 5′, 8-cyclo-2′-deoxyadenosine and their triphosphates were synthesized and purified by DEAE-Sephadex and reverse phase HPLC according to the procedures described previously [16]. Oligonucleotides were synthesized by Integrated DNA Technologies (IDT, Coralville, IA, USA). Radionucleotide, ^{32}P-ATP (6000 μCi/mmol) was purchased from PerkinElmer Inc (Boston, MA, USA). Micro Bio-Spin 6 chromatography columns were from Bio-Rad (Hercules, CA, USA). Human pol β and DNA ligase I (LIG I) were purified as described previously [34]. Human Pol η (polymerase domain) was provided by Dr. Wei Yang at National Institute of Diabetes and Digestive and Kidney Diseases (NIDDK)/National Institutes of Health (NIH) [22] (Supplementary Figure S1). All other standard chemical reagents were from Sigma–Aldrich (St. Louis, MO, USA) and Thermo Fisher Scientific (Pittsburgh, PA, USA).

2.2 Oligonucleotide substrates

Oligonucleotide substrates containing a 1 nt-gap were designed to mimic the 1 nt-gap intermediates formed during BER for testing the incorporation of cdAs and extension of the incorporated cdAs by DNA polymerases. The substrates were constructed by annealing the upstream primer (22 nt) without or with a cdA at the 3'-terminus and the downstream primer (23 nt) containing either a 5'-phosphate or 5'-phosphorylated tetrahydrofuran (THF) residue, an analog of deoxyribose phosphate (dRP) with the 46 nt template strand containing a dT or dC located at the 23rd or 24th nucleotide counted from the 3'-end. The molar ratio of the upstream primer, downstream primer, and the template is 1:2:2. The substrates were radiolabeled at the 5'-end of the upstream primer. To construct the substrates for testing the extension and ligation of incorporated cdAs, the upstream primer with a cdA at the 3'-terminus was generated by incubating 100 nM 1 nt-gap substrate containing a THF or phospahte at the 5'-end of the downstream primer with 50 nM pol β or pol η in the presence of 200 μM cdA in BER buffer containing 50 mM Tris-HCl, pH 7.5, 50 mM KCl, 0.1 mM EDTA, 0.1 mg/ml bovine serum albumin, and 0.01% Nonidet P-40 at 37°C for 30 min. The upstream primer was then subject to gel purification using 15% urea-denaturing polyacrylamide gel electrophoresis. The purified upstream primer with a 3' terminus cdA was annealed to the downstream primer and the template strand at a molar ratio of 1:2:2, creating a nicked substrate.

2.3 Enzymatic activity assays

The incorporation of cdAs by the DNA polymerases with the 1 nt-gap substrate was measured by incubating 25 nM substrates with increasing concentrations of DNA polymerases in the presence of 200 μM cdA or a fixed concentration of the DNA polymerases in the presence of increasing concentrations of cdA. The enzymes were incubated with the substrate at 37 °C for 30 minutes in 10 μl-reaction mixture containing 50 mM Tris-HCl, pH 7.5, 50 mM KCl, 0.1 mM EDTA, 0.1 mg/ml bovine serum albumin, and 0.01% Nonidet P-40. To test if an incorporated cdA can be further extended by DNA polymerases leading to a ligation product, the upstream primer with a 3-terminus cdA at the substrate was then incubated with various concentrations of DNA polymerases at 37°C for

30 min in BER buffer containing 50 mM Tris-HCl, pH 7.5, 50 mM KCl, 5 mM Mg^{2+}, 0.1 mM EDTA, 0.1 mg/ml bovine serum albumin, and 0.01% Nonidet P-40. To further examine if an incorporated cdA can be ligated at a nick by LIG I during BER, we incubated the nicked substrate containing a 3'-terminus cdA with increasing concentrations of LIG I in BER buffer containing 5 mM Mg^{2+} and 1 mM ATP at 37 °C for 30 minutes. Substrates and products were separated by 15% urea-denaturing polyacrylamide gel and detected by a phosphorimager. All experiments were repeated at least three times.

2.4 Steady-state kinetics of incorporation and extension of cdAs by pol β and pol η

The steady-state kinetics of the incorporation and extension of cdA opposite dT and dC by pol β and pol η were initially determined using various concentrations of 1 nt-gapped DNA substrates ranging from 5 nM to 50 nM with a fixed concentration of pol β (25 nM) or pol η (5–10 nM) in the presence of 200 μM cdA for its incorporation, and 50 μM dG for cdA extension. The kinetic studies were then performed by varying the concentrations of cdA (50 μM to 1 mM) in the presence of 25 nM pol β or 10 nM pol η for incorporation and using the varying concentration of dG (5–200 μM) in the presence of 25 nM pol β or 5 nM pol η for cdA extension. The cdA incorporation and extension products at different time intervals from 0 to 10 min or 15 min were determined and quantified, and the velocity of the polymerases at various substrate concentrations were obtained. The velocity and substrate concentrations were then analyzed using the enzyme kinetics module of Prism-GraphPad, version 6.03. The Michaelis-Menten constants, K_m, V_{max}, and k_{cat} values were obtained.

2.5 Molecular docking of cdA in the crystal structures of pol β and pol η

Protein structures were obtained from the protein data bank. The X-ray crystal structures of the pol β (PDB ID 5TBB) and pol η (PDB ID 4J9N) were chosen for the molecular docking analysis because of their high resolution [35, 36]. In addition, since pol β structure (PDB ID 5TBB) illustrates the interaction of the enzyme with a 1 nt-gap substrate, it can be used as a platform for molecular simulation of the incorporation of cdA with the 1 nt-gap substrate in our study. For the dT template of pol β structure, the 6th base was replaced with dT. Autodock vina [37] was used to dock the 5'R-cdA and 5'S-cdA to pol β and pol η. The structures were rendered using PyMol 2.1 [38].

3. Results

3.1 cdA can be incorporated into DNA by pol β and pol η

The repair polymerases, pol β and translesion polymerases such as pol η play an important role in mediating DNA lesion bypass during DNA replication and repair [39, 40]. Pol β can also incorporate an 8-oxoG to DNA during BER [41]. On the other hand, replication DNA polymerases have high fidelity of DNA synthesis and possess the 3'−5' exonuclease activity for its proofreading. We reason that pol β and translesion DNA polymerases can incorporate a cdA into DNA through their gap-filling synthesis during BER. To test this, we initially determined if DNA polymerases can incorporate cdAs by examining the incorporation of 5'R- and 5'-ScdA in the presence of increasing concentrations of pol β, pol η, pol θ, pol ν, and the replication polymerase, pol δ with the 1 nt-gap substrate without or with a 5'-phosphorylated THF. We found that pol β and pol η incorporated a comparable amount of

cdAs with the substrate. However, pol θ, pol ν, and Pol δ failed to incorporate cdAs (data not shown). Thus, we further characterized the cdA incorporation by pol β and pol η on the 1 nt-gap substrate with or without a dRP group that is represented by THF. The substrates represent the 1 nt gap intermediates formed before and after the dRP group is removed by pol β dRP lyase activity during BER. They were employed to test if the dRP group can affect the efficiency of cdA incorporation. We initially examined the incorporation of a 5'R- or 5'S-cdA by pol β on the 1-nt gap substrates containing a template dT with a 5′-phosphate or 5′-phosphorylated THF residue in the downstream primer (Figure 2). The results showed that increasing concentrations of pol β (10 nM-100 nM) incorporated 5'S-cdA and 5'R-cdA (200 μM) to fill in the 1 nt gap on the substrates with low efficiency (Figure 2A, lanes 2–5, 7–10, 12–15, 17–20). Pol β incorporated more cdA on the substrate containing a THF than the one without a THF (Figure 2A, compare lanes 2–5, 7–10 with lanes 12–15, 17–20). Pol β exhibited poor incorporation of 5'S-cdA on the gapped substrates generating only up to 5% and 1% incorporation product on the substrate with or without THF (Figure 2A, compare lanes 2–5 with lanes 7–10). The incorporation of 5'R-cdA by high concentrations of pol β also generated a small amount of a 2 nt insertion product on the substrates (Figure 2A, lanes 9–10 and 19–20), indicating that pol β extended 5'R-cdA leading to the incorporation of the nucleotide that was basepaired with the template dC. To determine if the concentration of cdA may also affect the efficiency of its incorporation, we examined cdA incorporation by pol β (50 nM) on the substrates in the presence of increasing concentrations of cdA (Figure 2B). The results showed that increasing concentrations of 5'S-cdA and 5'R-cdA (50 μM-500 μM) significantly stimulated the pol β incorporation of the nucleotides on the 1 ntgapped THF substrate (Figure 2B, lanes 2–5 and lanes 7–10). On the 1 nt-gapped substrate, increasing concentrations of cdA enhanced the pol β incorporation of 5'R-cdA (Figure 2B, lanes 17–20) but not the incorporation of 5'S-cdA (Figure 2B, lanes 12–15). In addition, at high concentrations of 5'R-cdA, pol β extended an inserted cdA to generate a cdA:C mismatch (Figure 2B, lanes 10, 18–20). The results indicate that pol β incorporated 5'R-cdA more efficiently than it inserted 5'S-cdA. The results also indicate that the 5'-sugar-phosphate significantly stimulated pol β incorporation of cdA (Figures 2A and 2B, compare lanes 2–5 with lanes 12–15 and lanes 7–10 with lanes 17–20). We then examined if pol η can also incorporate cdA to fill the 1 nt gap. We found that increasing concentrations of pol η (1 nM-50 nM) generated a significant amount of 1 nt insertion product from 5'R-cdA and 5'S-cdA on the substrates with or without a THF (Figure 3A, lanes 2–6, 8–12, 14–18, and 20–24). Moreover, we found that high concentrations of pol η inserted multiple cdA to misbasepair with the template nucleotides on the 1 nt-gapped substrates (Figure 3A, lanes 5–6, 11–12, 17–18, and 23–24). The results indicate that pol η extended an inserted cdA and continued to incorporate cdA to misbasepair with the template nucleotides. Similarly, increasing concentrations of 5'R-cdA and 5'S-cdA significantly stimulated the insertion of the damaged nucleotides in the presence of 20 nM pol η (Figure 3B, lanes 2–6, 8–12, 14–18, and 20–24). High concentrations of 5'S-cdA and 5'R-cdA also resulted in the extension of an inserted cdA and nucleotide misinsertion by pol η (Figure 3B, lanes 5–6, 11–12, 17–18, and 24). Interestingly, pol η did not show a significant difference in its incorporation of cdA on the substrate with or without THF (Figures 3A and 3B, compare lanes 2–6, 8–12 with lanes 14–18, lanes 20–24), indicating that the translesion DNA polymerase did not exhibit a preference for the 5'-sugar phosphate group. The results

suggest that pol η accommodated cdA lesions more efficiently in its active site than pol β, thereby facilitating the efficient incorporation of the damaged nucleotide. The results are also consistent with previous studies showing that pol η can readily bypass cdA lesions [16, 42, 43]

3.2 Pol β and pol η can misincorporate cdA opposite a template dC during BER.

It is reported that pol β and pol η can bypass oxidized DNA bases during DNA replication and BER [20, 22, 43]. However, the polymerases can perform nucleotide misinertion during lesion bypass [16, 20, 24, 43]. Since we found that pol β and pol η were able to extend 5'R- and 5'S-cdA, creating a cdA:dC mismatch at high concentrations of the polymerases or the nucleotides (Figure 2A, lanes 4–5, 9–10, and 19–20, Figure 2B, lanes 9–10 and 19–20, Figures 3, lanes 5–6, 11–12, 17–18, and 23–24), we then validated the incorporation of 5'R-cdA and 5'S-cdA to basepair with a template dC by pol β and pol η (Figure 4A and 4B). The results showed that with 200 μM cdATP, increasing concentrations of pol β at 1 nM-50 nM resulted in 5–60% of incorporation of 5'R-cdA and 5'S-cdA that basepaired with a dC on the substrates with or without a THF (Figure 4A, lanes 2–5, 7–10, 12–15, and 17–20). Similarly, in the presence of the same concentration of cdATP, 1–50 nM pol η led to the incorporation of 5–80% cdATP that basepaired with dC on the substrate with or without the THF residue (Figure 4B, lanes 2–6, 8–12, 14–18, and 20–24). We also found that pol β and pol η failed to incorporate cdATP to basepair with a dG (data not shown). The results indicate that pol β and pol η preferentially created a cdA:dC mismatch that may potentially lead to a transition mutation *in vivo*.

3.3 Incorporated cdA can be extended by repair DNA polymerases leading to the formation of the ligated repair product.

We then asked if an incorporated cdA can be further extended by pol β and pol η, thereby leading to the repair product and preventing DNA strand breaks during BER. We initially examined the extension of an incorporated cdA by pol β and pol η using a nicked substrate containing 5'R-cdA or 5'S-cdA at the 3'-end of the upstream primer. We found that increasing pol β (5 nM-25 nM) concentrations readily extended both 5'R-cdA and 5'S-cdA and inserted a dG to basepair with a template dC (Figure 5A, lanes 2–4, 6–8, 10–12, and 14–16). Similarly, the same concentrations of pol η efficiently extended 5'R-cdA and 5'S-cdA and inserted a dG (Figure 5B, lanes 2–4, 6–8, 10–12, and 14–16). Interestingly, we found that pol η at all concentrations still managed to incorporate dG that basepaired with the next template nucleotide, especially with the substrates containing a THF (Figure 5B, lanes 11–12 and 14–16). The results further indicated that pol β and pol η not only incorporated cdA but also readily extended the lesions and created nucleotide misincorporation facilitating the integration of cdA lesions into the genomic DNA. Since the integration of cdPu lesions in DNA may also be accomplished through the direct ligation of incorporated cdAs, which is the essential step for the completion of BER, next, we tested if a nick generated from the incorporated cdAs can be ligated by LIG I (Figure 6), DNA ligase that can be involved in both single-nucleotide and long-patch BER subpathway. We tested this by incubating the nicked substrate containing 5'S-cdA or 5'R-cdA at the 3' end of the upstream primer with increasing concentrations (5 nM-25 nM) of LIG I. We found that LIG I at 5 nM-25 nM resulted in 40%−90% ligation product (Figure 6, lanes 2–4, 6–8, 10–12, and 14–16),

which was comparable with the ligation product resulting from dA (87–93%) and dG (92% −97%)(Supplementary Figure S2) indicating that LIG I efficiently ligated the nick generated from the incorporated 5'R-cdA and 5'S-cdA. Our results suggest that cdA lesions can be incorporated into the human genome by repair DNA polymerases through BER.

3.4 Steady-state kinetics of pol β and pol η

To gain the new insights into the molecular mechanisms underlying the incorporation and extension of cdAs by pol β and pol η, we further performed the steady-state kinetic studies on the incorporation and extension of cdAs with different template nucleotides by pol β and pol η and determined the K_m, k_{cat}, and catalytic efficiency, k_{cat}/K_m for the enzymatic reactions (Table I and Table II). The kinetics studies were performed by varying the concentrations of cdAs and DNA substrates (Table I and II). The results showed that pol β incorporation of 5'R-cdA opposite dT on the substrates without or with a THF exhibited a high $K_{m,cdA\text{-}dT}$ of 122–141 μM with low $k_{cat,cdA\text{-}dT}$ of 8.2–18.5 × 10^{-4} s^{-1} and $k_{cat,cdA\text{-}dT}/K_{m,cdA\text{-}dT}$ of 6.7–13.1 × 10^{-6} μM^{-1} s^{-1} (Table I). In contrast, the polymerase exhibited $K_{m,DNA\text{-}dT}$ of 3.5–8.0 × 10^{-2} μM with $k_{cat,DNA\text{-}dT}$ ranging from 7.0 to 23 × 10^{-4} S^{-1} and $k_{cat,DNA\text{-}dT}/K_{m,DNA\text{-}dT}$ of 2.0–2.9 × 10^{-2} μM^{-1} s^{-1} (Table I). The efficiency for the polymerase to incorporate cdA opposite dT with a THF is ~1.5–2-fold of that without the residue (Table I). However, we could not obtain the K_m and k_{cat} for 5'-ScdA because no nucleotide incorporation could be detected. The $K_{m,cdA\text{-}dC}$ for 5'R-cdA and 5'S-cdA on the substrates without or with THF ranged from 193 μM to 398 μM (Table I). The $k_{cat,cdA\text{-}dC}$ for 5'R-cdA and 5'S-cdA was 12–22 ×10^{-4} s^{-1} (Table I). The $k_{cat,cdA\text{-}dC}/K_{m,cdA\text{-}dC}$ was 4.1–6.2 × 10^{-6} μM^{-1} s^{-1}. However, both of $K_{m,cdA\text{-}dC}$ and $k_{cat,cdA\text{-}dC}$ were increased compared with $K_{m,cdA\text{-}dT}$ and $k_{cat,cdA\text{-}dT}$, thereby leading to similar catalytic efficiency with that of cdA incorporation opposite dT (Table I). Pol β exhibited a lower $K_{m,DNA\text{-}dC}$ (1.2–5.8 × 10^{-2} μM) than $K_{m,DNA\text{-}dT}$ (3.5–8 × 10^{-2} μM) and higher catalytic efficiency, $k_{cat,DNA\text{-}dC}/K_{m,DNA\text{-}dC}$ (3.3–6.7 × 10^{-2} μM^{-1} s^{-1}) than $k_{cat,DNA\text{-}dT}/K_{m,DNA\text{-}dT}$ (3.4–6.64 × 10^{-2} μM^{-1} s^{-1})(Table I). The catalytic efficiency for pol β to incorporate 5'R-cdA and 5'S-cdA opposite dC was ~1.5–3fold of that opposite dT (Table I). The kinetics from cdA also showed that pol β exhibited higher efficiency to incorporate 5'R-cdA opposite dT on the DNA substrate with THF than without the residue (Table I). The $K_{m,cdA\text{-}dT}$ for the enzyme to extend 5'R- and 5'S-cdA was lower than $K_{m,cdA}$dC (Table I). However, $k_{cat,cdA\text{-}dT}$ was higher than $k_{cat,cdA\text{-}dC}$ (Table I). This led to $k_{cat,cdA\text{-}dT}/K_{m,cdA\text{-}dT}$, which was 3.6–6-fold higher than $k_{cat,cdA\text{-}dC}/K_{m,cdA\text{-}dC}$ (Table I). In contrast, $k_{cat,DNA\text{-}dT}/K_{m,DNA\text{-}dT}$ was 7–8-fold lower than $k_{cat,cdA\text{-}dC}/K_{m,cdA\text{-}dC}$ (Table I). The results indicate that pol β managed to incorporate 5'R-cdA opposite dT on the 1 nt gap substrates with higher catalytic efficiency on the substrate with a THF, and the enzyme could also incorporate 5'R-cdA and 5'S-cdA opposite dC. The results further suggest that the incorporation of cdA during BER can simultaneously introduce the damaged nucleotides and mismatches to cause DNA damage and mutagenesis *in vivo*. Pol η did not exhibit a significant difference in the catalytic efficiency to incorporate 5'R- and 5'S-cdA opposite dT and dC (Table II). The enzyme exhibited a high $K_{m,cdA\text{-}dT}$ (62–158 μM) with a low $k_{cat,cdA\text{-}dT}$ (25.8–38.3 × 10^{-4} s^{-1}) and relatively high $K_{m,cdA\text{-}dC}$ (91–222 μM) and $k_{cat,cdA\text{-}dC}$ (114–155 × 10^{-4} s^{-1}). The results led to the catalytic efficiency of $k_{cat,cdA\text{-}dT}/K_{m,cdA\text{-}dT}$, 2.4–4.1 × 10^{-5} μM^{-1} s^{-1} and $k_{cat,cdA\text{-}dC}/K_{m,cdA\text{-}dC}$, 7–12.5 × 10^{-5} μM^{-1} s^{-1}. The $K_{m,DNA}$ varies from 1.3 to 4.4 × 10^{-2} μM with $k_{cat,DNA}$ ranging from 10 to

31×10^{-4} μM^{-1} s^{-1} and $k_{cat,DNA\text{-}dT}/K_{m,DNA\text{-}dT}$ of 4.5–10×10^{-2} μM^{-1} s^{-1} (Table II). The kinetics results indicated that the polymerase exhibited ~3-fold higher catalytic efficiency to incorporate cdA opposite dC than dT (Table II). The results further indicate that the polymerase preferentially incorporated cdA opposite dC. For the extension of 5'R- and 5'S-cdA opposite dT, pol η exhibited $K_{m,cdA\text{-}dT}$ of 2.8–7.4 μM and $K_{m,DNA\text{-}dT}$ of 1–1.2 $\times 10^{-2}$ μM, $k_{cat,cdA\text{-}dT}$ of 25–31.1 $\times 10^{-4}$ s^{-1}, and $k_{cat,DNA\text{-}dT}$ of 159–197 $\times 10^{-4}$ s^{-1}, leading to $k_{cat,cdA\text{-}dT}/K_{m,cdA\text{-}dT}$ of 61–110 × 10–5 μM^{-1} s^{-1} and $k_{cat,DNA\text{-}dT}/K_{m,DNA\text{-}dT}$ of 158–163 $\times 10^{-2}$ μM^{-1} s^{-1} (Table II). For the extension of 5'R- and 5'S-cdA opposite dC, the polymerase exhibited $K_{m,cdA\text{-}dC}$ of 4.0–7.4 μM and $K_{m,DNA\text{-}dC}$ of 6.8–12.5 $\times 10^{-2}$ μM, $k_{cat,cdA\text{-}dC}$ of 15–25 $\times 10^{-4}$ s^{-1} and $k_{cat,DNA\text{-}dT}$ of 884–1622 $\times 10^{-4}$ s^{-1}, leading to $k_{cat,cdA\text{-}dC}/K_{m,cdA\text{-}dC}$ of 34–38 $\times 10^{-5}$ μM^{-1} s^{-1} and $k_{cat,DNA\text{-}dC}/K_{m,DNA\text{-}dC}$ of 130 $\times 10^{-2}$ μM^{-1} s^{-1}, respectively (Table II). The catalytic efficiency for the enzyme to extend cdA is 2.4–41-fold of that for the nucleotide incorporation (Table II). In addition, pol η exhibited significantly higher efficiency of incorporation and extension of cdA than that pol β (compare Table II and Table I), demonstrating its profound role in incorporating and extending cdAs and introducing mismatches into DNA.

3.5 Repair DNA polymerases accommodate cdA lesions in their active sites to facilitate the phosphodiester bond formation and nucleotide incorporation.

To further gain the mechanistic insights into how pol β and pol η incorporated cdA, creating a mismatch during BER, we then conducted a molecular docking analysis on the structures of the DNA polymerases (pol β, PDB5TBB [35], pol η PDB4J9N [36] that were docked with cdA using Autodock vina and PyMOL 2.1. We found that in the active site of pol β, the base of 5'R-cdA was orientated facing dT or dC compared with dA:dT and dG:dC base pair (Figure 7A, 7B, panels a-b). In contrast, 5'S-cdA exhibited a distorted configuration that pulled out the base away from the template dT and dC (Figure 7B, panels a-b, bottom). However, our docking analysis failed to predict any hydrogen bond formation between cdA and the template dT or dC (data not shown). The results are consistent with those showing that pol β performed the incorporation of 5'R-cdA and poor incorporation of 5'S-cdA (Figures 2 and 4). At pol η active site, only 5'S-cdA was oriented to face toward the template dT (Figure 7C, panel a, bottom). 5'R-cdA and 5'S-cdA were pulled out away from the template dT and dC (Figure 7C, panels a-b). No hydrogen bonds were predicted between cdA and the template bases (data not shown). Overlay of cdATP on dA opposite a template dT in pol β revealed that the base of 5'R-cdATP was aligned well with that of dA (Figure 7D, panel a). However, the phosphate groups failed to align with the 5'-phosphate and pyrophosphate from dATP (Figure 7D, panel a). The base and phosphate groups of 5'S-cdATP were turned away from dATP (Figure 7D, panel a). 5'R- and 5'S-cdATP in pol η were positioned away from the base of dATP. However, their γ- and β-phosphates were aligned well with the pyrophosphates released from dATP (Figure 7D, panel b). We then looked into the amino acid residues involved in facilitating the incorporation of 5'R- and 5'S-cdA by pol β and pol η (Figure 7E). For pol β, F272 and Y271 in the α-helix were positioned parallel or perpendicular to the base of 5'R-cdA and 5'S-cdA (Figure 7E, panels a-b). G179 was in proximity with the β-phosphate of 5'R-cdA but not with that of 5'S-cdA (Figure 7E, panels a-b). D190 and R258 appeared to coordinate with two magnesium ions, which interacted with the phosphate groups of cdAs (Figure 7E, panels a-b). For pol η, F18

was parallel with the sugar and base rings of 5'R-cdA and 5'S-cdA, respectively (Figure 7E, panels c-d). D115 and D13 were coordinated with magnesium ions, and K231 and R55 were coordinated with the β and γ phosphate groups of cdA (Figure 7E, panels c-d). The results suggest that the hydrophobic interaction between the bases of cdA and hydrophobic amino acids, along with the coordinated phosphates and magnesium ions, mediated the cdA incorporation by the repair DNA polymerases.

4. Discussion

In this study, for the first time, we discovered that human repair DNA polymerases, pol β and pol η incorporated 5'R-cdA and 5'S-cdA into duplex DNA through BER (Figures 2–4). We demonstrated that the incorporated cdA lesions were efficiently extended by repair DNA polymerases and ligated into duplex DNA (Figures 5–6). Further analysis on the catalytic efficiency of cdA incorporation and extension by pol β and pol η showed that $K_{m,cdA\text{-}dT}$ for pol β 5'R-cdA incorporation on the 1 nt gap substrate was ~14–16-fold higher than $K_{m,dA\text{-}dT}$ and ~2-fold higher than $K_{m,dCTP}$ of rat pol β (Table I) [44, 45]. $K_{m,DNA\text{-}dT}$ for pol β 5'R-cdA incorporation is 1.5-3-fold lower than $K_{m,DNA\text{-}dTTP}$ [44]. The $K_{m,cdA\text{-}dT}$ of pol η is 230–266-fold higher than $K_{m,dATP}$ for correct nucleotide insertion and ~4–5-fold higher than $K_{m,dCTP}$ for incorrect nucleotide insertion (Table II) [46]. However, our results showed that the $k_{cat,cdA\text{-}dT}$ and catalytic efficiency, $k_{cat,cdA}dT/K_{m,cdA\text{-}dT}$ of pol β was ~432–1000-fold and ~6700–13000-fold lower than its correct nucleotide insertion (Table I) [44]. Similarly, $k_{cat,cdA\text{-}dT,}$ and $k_{cat}/K_{m,\ cdA\text{-}dT}$ for pol η were ~60–90-fold and ~1875–3750-fold lower than correct nucleotide insertion (Table II) [46]. However, $k_{cat,cdATP\text{-}dC}$ of pol η was only ~16–24-fold lower than that of $k_{cat,dATP\text{-}dC}$ (Table II) [46]. The catalytic efficiency, $k_{cat}/K_{m,cdA\text{-}dC}$ was ~18–34-fold lower than $k_{cat}/K_{m,dCTP}$. The results indicated that pol β and pol η exhibited poor interaction with cdATP. The results further suggest that the DNA polymerases attempted to increase the efficiency of the catalysis of cdA incorporation by lowering $K_{m,DNA}$. Since our molecular docking results showed that no hydrogen bond formed between template dT, dC, and cdAs in pol β and pol η (Figure 7), it is conceivable that the polymerases could adopt a unique conformation to facilitate the catalysis of cdA incorporation but also trap themselves on the DNA substrates. Analysis on the rate of the extension of the 3'-terminus cdA that basepaired with dT by the polymerases showed that the $K_{m,cdA\text{-}T}$ for pol β extension of cdAs was ~ 227–336-fold and ~100280-fold higher than its extension of dG and an 8-oxodG (Table I) [33]. In contrast, $k_{cat,cdA\text{-}T}$ for pol β cdA extension was ~122–176-fold and ~8–12-fold lower than its extension of dG and 8oxodGs, leading to the catalytic efficiency that was ~2.5–4 $\times 10^4$-fold and 774–1255-fold lower than its extension of the undamaged and damaged nucleotides (Table I) [33]. The $K_{m,\ cdA\text{-}dT}$ for pol η extension of cdAs was lower than that for pol β (Table I and Table II), leading to ~3.6–15fold higher catalytic efficiency than that of pol β (Table I and Table II). The results indicate that pol η promoted the incorporation of cdA lesions in DNA more efficiently than pol β by extending the damaged nucleotides. The results further suggest that the accumulation of cdPu lesions in the genome can be aggravated by their incorporation through repair DNA polymerases during BER, along with the low efficiency of their removal by NER [13]. Thus, we suggest a potential role of repair DNA polymerases in causing the accumulation of cdPu lesions in the genome by incorporating oxidized nucleotides.

Surprisingly, our results also showed that the polymerases led to cdA:dC mismatch (Figure 2–6). This may potentially result in a transition mutation *in vivo*. A previous study indicates that *E. Coli* repair DNA polymerase I (Klenow fragment) can incorporate 5′S-cdATP opposite dT. In contrast, it incorporates 5′R-cdATP opposite a template dC [47], demonstrating similarity between the bacterial repair DNA polymerase and human DNA repair polymerases in misincorporating cdA into genomic DNA. Our results are consistent with our previous finding showing that high concentrations of pol β can also misincorporate dC to bypass a template cdA [20]. Here, we further demonstrate that the human repair DNA polymerases can also perform nucleotide misinsertion through its direct incorporation of cdPus. Our results suggest that the incorporation of cdA by repair DNA polymerases can potentially serve as an alternative mechanism to induce oxidative DNA damage and its-resulted mutations in the genome. Considering the low efficiency of repair of cdPu lesions by NER, the mutagenic effects resulting from cdA:dC misbasepair may lead to more severe adverse biological effects than other types of base lesions.

Our results also showed that pol β and pol η exhibited a difference in incorporating cdA lesions. We found that pol β incorporated much more 5’R-cdA than 5’S-cdA (Figures 2 and 4A). This suggests that 5’R-cdA adopted a configuration that favored its incorporation by pol β. The results are consistent with those from our previous study showing that the pol β can efficiently bypass a template 5’R-cdA but not 5’S-cdA [20]. Our molecular docking analysis results further provided several structural insights into the underlying mechanisms. First, the base of 5’R-cdA but not 5’-SdA was oriented to face the template nucleotide in the pol β active site (Figures 7B and 7D, panel a). Second, although the base of 5’R-cdA did not form hydrogen bonds with that of the template dT (data not shown), it was oriented to parallel with the side chain of F272 (Figure 7D, panel a), suggesting a hydrophobic interaction between the rings of F272 and adenine of 5’R-cdA. Third, for both 5’R-cdA and 5’S-cdA, Y271 were positioned to be perpendicular to the base (Figure 7E, panels a-b), indicating the loss of its hydrophobic interaction with the cdA base. Fourth, structural overlay suggested that R258, D190, and G179 were responsible for coordinating with magnesium and phosphates to facilitate the catalysis of 5’R-cdA incorporation (Figure 7E, panel a). The disappearance of G179 in the presence of 5’ScdA (Figure 7E, panel b) suggested that G179 coordinated with the phosphates to facilitate the nucleophilic attack from the 3’-OH group. On the other hand, in the active site of pol η, the base of 5’R-cdA and 5’S-cdA was turned away from the template dT and dC (Figure 7C). Although 5’S-cdA was oriented to face to dT, its incorporation by pol η exhibited little difference from that of 5’R-cdA (Figure 3). A structural overlay between the β- and γ-phosphate of cdA and that of dA (Figure 7D, panel b) in the active site of pol η suggested that the coordinated phosphates of cdA mediated the catalysis of cdA incorporation. This appeared to be mediated by K231 and R55 and magnesium ions coordinated by D13 and D115 (Figure 7E, panels c-d). In addition, the hydrophobic interaction between F18 and in the rings of sugar of 5’R-cdA and adenine could also be involved in stabilizing the base and orientation of the phosphates facilitating the catalysis of cdA incorporation. The mechanistic insights can be validated using X-ray crystallography of pol β and pol η with the mutations of critical amino acids in their catalytic sites. The studies will further reveal the enzyme-substrate interaction and catalysis for cdA incorporation of the polymerases.

Our results suggest that the incorporation of cdA by pol β and pol η was mediated by the nucleophilic attack between the 3'-hydroxy group of the last nucleotide of the primer and α-phosphate of cdATP in the absence of hydrogen bonds. It appeared that the hydrophobic interaction between cdA and template bases and base stacking facilitated the proximity between the 3'-hydroxyl group and the α-phosphate, promoting the nucleophilic attack and cdA incorporation. The results suggest that the nucleophilic attack from the 3'-hydroxyl group to the α-phosphate of 5'R-and 5'S-cdA played a predominant role in mediating the incorporation of cdA. However, the cdA:dC misbasepair generated by pol β and pol η (Figure 4) further suggesting that the loss of the hydrogen bond between cdA and dT resulted in the mismatches, demonstrating that the hydrogen bonding was essential for maintaining the fidelity of the repair DNA polymerases.

A variety of oxidized nucleotides including cdPus and 8-oxodG among others can be generated in the DNA or the nucleotide pool [48, 49]. However, it remains unknown how much cdPus can be generated from the nucleotide pool in human cells. It has been shown that free dGTP are oxidized with an 8–9-fold higher frequency than dGMP [30] indicating that dGTP is more susceptible to oxidation than dGMP *in vivo*. It is estimated that the concentration of 8-oxodG ranges from 0.2 to 2 μM in the nucleotide pool of mitochondria in rat tissues under physiological conditions [50]. Considering the bigger size of nucleus than mitochondria, it is possible that more 8-oxodGTP can be generated in the nucleotide pool of the nucleus. Similar to the cellular production of 8-oxodGTP, it is conceivable that more cdPu triphosphate may also be generated from the oxidation of the nucleotide pool than from direct oxidation of deoxypurines in double-strand DNA. It has been shown that there are approximately 10,000 8-oxodGs and 180–320 cdPus generated in the genomic DNA of mammalian cells and tissues per day [51]. Interestingly, a previous study has shown that pol β incorporates 8-oxodGTP at a low catalytic efficiency, $k_{cat}/K_{m,8\text{-oxodGTP}}$ of 130×10^{-5} min^{-1} μM^{-1} (2×10^{-5} s^{-1} μM^{-1}) [52]. Our result showed that $k_{cat}/K_{m,cdA}$ for pol β and pol η to incorporate cdA is 6.7–13.1 $\times 10^{-6}$ s^{-1} μM^{-1} and 2.4–4.1 $\times 10^{-5}$ s^{-1} μM^{-1}, respectively (Table I and II) that are comparable with the $k_{cat}/K_{m,8\text{-oxodGTP}}$. Thus, we suggest that pol β and pol η can play a significant role in promoting the accumulation of cdA in the genome. The contribution of cdPus lesions in DNA from the oxidized nucleotide pool needs to be further determined by examining the incorporation of cdGTPs and cdATPs by different repair DNA polymerases *in vitro* and *in vivo*. Moreover, since cdPus incorporated by repair DNA polymerases during BER can be recognized and removed by NER [13], it is possible that BER and NER can crosstalk to govern the incorporation of cdPu lesions. A recent study has shown that cdPu lesions can inhibit the repair of an AP site by BER in mammalian cells [53] suggesting that the removal of cdPus by NER can modulate BER efficiency. The coordination between BER and NER pathways in governing the accumulation and removal of cdPu lesions and base lesions needs to be further explored in the future.

cdPu lesions are associated with the etiology of breast cancer. This notion is supported by the fact that more cdPu lesions can be induced by oxidative stress in several breast cancer cell lines than normal cells [54]. This is because cancer cells proliferate more quickly than normal cells and can generate high level of H_2O_2-mediated oxidative stress [55]. Interestingly, cdPus may also be involved in the treatment of solid tumors by the antitumor drug, Tirapazamine (TPZ) [56]. In TPZ-treated hypoxic cells, the amount of

cdA and cdGs are significantly increased suggesting that cdPus lesions mediate cancer cell killing of TPZ [56]. Moreover, since nucleotide analogs are routinely used as drugs for cancer therapy [57–59], our discovery of the incorporation of cdA lesions in DNA by repair DNA polymerase suggests that cdPus can also be developed into a new nucleotide analog for cancer treatment. This is because, first, a single cdA lesion can efficiently inhibit DNA replication polymerases and RNA polymerase and the DNA binding of the TATA box-binding proteins [10, 14, 17], thereby inhibiting both DNA replication and gene transcription in cancer cells. Second, cdPu lesions are poorly repaired by NER leading to their accumulation in the genome [5]. This may inhibit cancer cell growth and progression. Finally, the misincorporation of cdPu lesions in DNA can potentially cause mutations during their incorporation and lesion bypass in cancer cells, thereby attenuating cancer cell survival.

In summary, in this study, we have discovered that the incorporation of cdA lesions by human repair DNA polymerases, pol β, and pol η. We showed that pol β and pol η not only incorporated the lesions but also created a cdA:dC mismatch. Moreover, the incorporated cdA lesions can be fully extended by pol β and ligated by LIG I, suggesting that the lesion can be readily embedded in the human genome. Using steady-state kinetics and molecular docking analysis, we provided new mechanistic insights into the mechanisms underlying cdA incorporation by pol β and pol η.

Supplementary Material

Refer to Web version on PubMed Central for supplementary material.

Acknowledgments

We thank Dr. Wei Yang at NIDDK/NIH for providing purified human pol η and critical comments. We thank Fei Qu for her technical assistance. This study is supported by NIHR01ES023569 to Y. L. P.S.T. is supported by Florida International University Dissertation Year Fellowship.

References

[1]. Instability Lindahl T. and decay of the primary structure of DNA. Nature. 1993;362:709–15. [PubMed: 8469282]

[2]. Cadet J, Delatour T, Douki T, Gasparutto D, Pouget JP, Ravanat JL, et al. Hydroxyl radicals and DNA base damage. Mutat Res. 1999;424:9–21. [PubMed: 10064846]

[3]. Dizdaroglu M Measurement of radiation-induced damage to DNA at the molecular level. Int. J. Radiat Bio. 1992;61:175–83. [PubMed: 1351904]

[4]. Jaruga P, Dizdaroglu M. 8,5'-Cyclopurine-2'-deoxynucleosides in DNA: mechanisms of formation. DNA Repair (Amst). 2008;7:1413–25. [PubMed: 18603018]

[5]. Brooks PJ. The 8,5'-cyclopurine-2'-deoxynucleosides: candidate neurodegenerative DNA lesions in xeroderma pigmentosum, and unique probes of transcription and nucleotide excision repair. DNA Repair (Amst). 2008;7:1168–79. [PubMed: 18495558]

[6]. Chatgilialoglu C, Bazzanini R, Jimenez LB, Miranda MA. (5'S)- and (5'R)-5',8-cyclo-2'deoxyguanosine: mechanistic insights on the 2'-deoxyguanosin-5'-yl radical cyclization. Chem Res Toxicol. 2007;20:1820–4. [PubMed: 17988100]

[7]. Wang Y Bulky DNA lesions induced by reactive oxygen species. Chem Res Toxicol. 2008;21:276–81. [PubMed: 18189366]

[8]. Chatgilialoglu C, D'Angelantonio M, Kciuk G, Bobrowski K. New insights into the reaction paths of hydroxyl radicals with 2'-deoxyguanosine. Chem Res Toxicol. 2011;24:2200–6. [PubMed: 21939266]

[9]. Cadet J, Douki T, Gasparutto D, Ravanat JL. Oxidative damage to DNA: formation, measurement and biochemical features. Mutat Res. 2003;531:5–23. [PubMed: 14637244]

[10]. Brooks PJ, Wise DS, Berry DA, Kosmoski JV, Smerdon MJ, Somers RL, et al. The oxidative DNA lesion 8,5'-(S)-cyclo-2'-deoxyadenosine is repaired by the nucleotide excision repair pathway and blocks gene expression in mammalian cells. J Biol Chem. 2000;275:2235562.

[11]. Das RS, Samaraweera M, Morton M, Gascon JA, Basu AK. Stability of N-glycosidic bond of (5'S)-8,5'-cyclo-2'-deoxyguanosine. Chem Res Toxicol. 2012;25:2451–61. [PubMed: 23025578]

[12]. Dizdaroglu M, Jaruga P, Rodriguez H. Identification and quantification of 8,5'-cyclo-2'deoxy-adenosine in DNA by liquid chromatography/ mass spectrometry. Free Radic Biol Med. 2001;30:774–84. [PubMed: 11275477]

[13]. Kropachev K, Ding S, Terzidis MA, Masi A, Liu Z, Cai Y, et al. Structural basis for the recognition of diastereomeric 5',8-cyclo-2'-deoxypurine lesions by the human nucleotide excision repair system. Nucleic Acids Res. 2014;42:5020–32. [PubMed: 24615810]

[14]. Kuraoka I, Bender C, Romieu A, Cadet J, Wood RD, Lindahl T. Removal of oxygen freeradical-induced 5',8-purine cyclodeoxynucleosides from DNA by the nucleotide excision-repair pathway in human cells. Proc Natl Acad Sci U S A. 2000;97:3832–7. [PubMed: 10759556]

[15]. Abraham J, Brooks PJ. Divergent effects of oxidatively induced modification to the C8 of 2'deoxyadenosine on transcription factor binding: 8,5'(S)-cyclo-2'-deoxyadenosine inhibits the binding of multiple sequence specific transcription factors, while 8-oxo-2'-deoxyadenosine increases binding of CREB and NF-kappa B to DNA. Environ Mol Mutagen. 2011;52:287–95. [PubMed: 20872830]

[16]. Chatgilialoglu C, Ferreri C, Geacintov NE, Krokidis MG, Liu Y, Masi A, et al. 5',8Cyclopurine Lesions in DNA Damage: Chemical, Analytical, Biological, and Diagnostic Significance. Cells. 2019;8. [PubMed: 31861404]

[17]. Marietta C, Gulam H, Brooks PJ. A single 8,5'-cyclo-2'-deoxyadenosine lesion in a TATA box prevents binding of the TATA binding protein and strongly reduces transcription in vivo. DNA Repair (Amst). 2002;1:967–75. [PubMed: 12531024]

[18]. You C, Swanson Al Fau - Dai X, Dai X Fau - Yuan B, Yuan B Fau - Wang J, Wang J Fau - Wang Y, Wang Y. Translesion synthesis of 8,5'-cyclopurine-2'-deoxynucleosides by DNA polymerases. J Biol Chem. 2013;288:28548–56 LID - 10.1074/jbc.M113.480459 [doi]. [PubMed: 23965998]

[19]. Xu M, Lai Y, Jiang Z, Terzidis MA, Masi A, Chatgilialoglu C, et al. A 5', 8-cyclo-2'deoxypurine lesion induces trinucleotide repeat deletion via a unique lesion bypass by DNA polymerase beta. Nucleic Acids Res. 2014;42:13749–63. [PubMed: 25428354]

[20]. Jiang Z, Xu M, Lai Y, Laverde EE, Terzidis MA, Masi A, et al. Bypass of a 5',8-cyclopurine2'-deoxynucleoside by DNA polymerase beta during DNA. DNA Repair (Amst). 2015;33:24–34. [PubMed: 26123757]

[21]. Walmacq C, Wang L, Chong J, Scibelli K, Lubkowska L, Gnatt A, et al. Mechanism of RNA polymerase II bypass of oxidative cyclopurine DNA lesions. Proc Natl Acad Sci U S A. 2015;112:E410–9. [PubMed: 25605892]

[22]. Weng PJ, Gao Y, Gregory MT, Wang P, Wang Y, Yang WA- O. Bypassing a 8,5'-cyclo-2'deoxyadenosine lesion by human DNA polymerase eta at. Proc Natl Acad Sci U S A. 2018;115:10660–5. [PubMed: 30275308]

[23]. Kuraoka I, Robins P Fau - Masutani C, Masutani C Fau - Hanaoka F, Hanaoka F Fau - Gasparutto D, Gasparutto D Fau - Cadet J, Cadet J Fau - Wood RD, et al. Oxygen free radical damage to DNA. Translesion synthesis by human DNA polymerase. J Biol Chem. 2001;276:49283–8. [PubMed: 11677235]

[24]. Swanson AL, Wang J Fau - Wang Y, Wang Y. Accurate and efficient bypass of 8,5'cyclopurine-2'-deoxynucleosides by human. Chem Res Toxicol. 2012;25:1682–91. [PubMed: 22768970]

[25]. Pednekar V, Weerasooriya S Fau - Jasti VP, Jasti Vp Fau - Basu AK, Basu AK. Mutagenicity and genotoxicity of (5'S)-8,5'-cyclo-2'-deoxyadenosine in. Chem Res Toxicol. 2014;27:200–10. [PubMed: 24392701]

[26]. Kirkali G, de Souza-Pinto NC, Jaruga P, Bohr VA, Dizdaroglu M. Accumulation of (5'S)-8,5'cyclo-2'-deoxyadenosine in organs of Cockayne syndrome complementation group B gene knockout mice. DNA Repair (Amst). 2009;8:274–8. [PubMed: 18992371]

[27]. Wang J, Clauson CL, Robbins PD, Niedernhofer LJ, Wang Y. The oxidative DNA lesions 8,5'-cyclopurines accumulate with aging in a tissue-specific manner. Aging Cell. 2012;11:714–6. [PubMed: 22530741]

[28]. Wang J, Yuan B, Guerrero C, Bahde R, Gupta S, Wang Y. Quantification of oxidative DNA lesions in tissues of Long-Evans Cinnamon rats by capillary high-performance liquid chromatography-tandem mass spectrometry coupled with stable isotope-dilution method. Anal Chem. 2011;83:2201–9. [PubMed: 21323344]

[29]. Rai P Oxidation in the nucleotide pool, the DNA damage response and cellular senescence: Defective bricks build a defective house. Mutat Res. 2010;703:71–81. [PubMed: 20673809]

[30]. Kamiya H, Kasai H. Formation of 2-hydroxydeoxyadenosine triphosphate, an oxidatively damaged nucleotide, and its incorporation by DNA polymerases. Steady-state kinetics of the incorporation. J Biol Chem. 1995;270:19446–50. [PubMed: 7642627]

[31]. Kasai H, Nishimura S. Hydroxylation of deoxyguanosine at the C-8 position by ascorbic acid and other reducing agents. Nucleic Acids Res. 1984;12:2137–45. [PubMed: 6701097]

[32]. Macpherson P, Barone F, Maga G, Mazzei F, Karran P, Bignami M. 8-oxoguanine incorporation into DNA repeats in vitro and mismatch recognition by MutSalpha. Nucleic Acids Res. 2005;33:5094–105. [PubMed: 16174844]

[33]. Whitaker AM, Smith MR, Schaich MA, Freudenthal BD. Capturing a mammalian DNA polymerase extending from an oxidized nucleotide. Nucleic Acids Res. 2017;45:6934–44. [PubMed: 28449123]

[34]. Beaver JM, Lai Y, Xu M, Casin AH, Laverde EE, Liu Y. AP endonuclease 1 prevents trinucleotide repeat expansion via a novel mechanism during base excision repair. Nucleic Acids Res. 2015;43:5948–60. [PubMed: 25990721]

[35]. Reed AJ, Vyas R, Raper AT, Suo Z. Structural Insights into the Post-Chemistry Steps of Nucleotide Incorporation Catalyzed by a DNA Polymerase. J Am Chem Soc. 2017;139:465–71. [PubMed: 27959534]

[36]. Zhao Y, Gregory MT, Biertumpfel C, Hua YJ, Hanaoka F, Yang W. Mechanism of somatic hypermutation at the WA motif by human DNA polymerase eta. Proc Natl Acad Sci U S A. 2013;110:8146–51. [PubMed: 23630267]

[37]. Trott O, Olson AJ. AutoDock Vina: improving the speed and accuracy of docking with a new scoring function, efficient optimization, and multithreading. J Comput Chem. 2010;31:455–61. [PubMed: 19499576]

[38]. L S. The PyMOL Molecular Graphics System. Schrödinger, Inc: New York, NY.

[39]. Vaisman A, Woodgate R. Translesion DNA polymerases in eukaryotes: what makes them tick? Crit Rev Biochem Mol Biol. 2017;52:274–303. [PubMed: 28279077]

[40]. Crespan E, Pasi E, Imoto S, Hubscher U, Greenberg MM, Maga G. Human DNA polymerase beta, but not lambda, can bypass a 2-deoxyribonolactone lesion together with proliferating cell nuclear antigen. ACS Chem Biol. 2013;8:336–44. [PubMed: 23101935]

[41]. Caglayan M, Horton JK, Dai DP, Stefanick DF, Wilson SH. Oxidized nucleotide insertion by pol beta confounds ligation during base excision repair. Nat Commun. 2017;8:14045. [PubMed: 28067232]

[42]. Swanson AL, J W, Y W. Accurate and efficient bypass of 8,5'-cyclopurine-2'deoxynucleosides by human and yeast DNA polymerase η. Chem Res Toxicol. 2012;25:168291 LID - 10.021/tx3001576 [doi].

[43]. You C, Swanson AL, Dai X, Yuan B, Wang J, Wang Y. Translesion synthesis of 8,5'cyclopurine-2'-deoxynucleosides by DNA polymerases eta, iota, and zeta. J Biol Chem. 2013;288:28548–56. [PubMed: 23965998]

[44]. Beard WA, Osheroff WP, Prasad R, Sawaya MR, Jaju M, Wood TG, et al. Enzyme-DNA interactions required for efficient nucleotide incorporation and discrimination in human DNA polymerase beta. J Biol Chem. 1996;271:12141–4. [PubMed: 8647805]

[45]. Chagovetz AM, Sweasy JB, Preston BD. Increased activity and fidelity of DNA polymerase beta on single-nucleotide gapped DNA. J Biol Chem. 1997;272:27501–4. [PubMed: 9346877]

[46]. Washington MT, Johnson RE, Prakash L, Prakash S. The mechanism of nucleotide incorporation by human DNA polymerase eta differs from that of the yeast enzyme. Mol Cell Biol. 2003;23:8316–22. [PubMed: 14585988]

[47]. Kamakura N, Yamamoto J, Brooks PJ, Iwai S, Kuraoka I. Effects of 5',8cyclodeoxyadenosine triphosphates on DNA synthesis. Chem Res Toxicol. 2012;25:2718–24. [PubMed: 23146066]

[48]. Kasai H, Nishimura S. Hydroxylation of the C-8 position of deoxyguanosine by reducing agents in the presence of oxygen. Nucleic Acids Symp Ser. 1983:165–7. [PubMed: 6664853]

[49]. Nakabeppu Y Cellular levels of 8-oxoguanine in either DNA or the nucleotide pool play pivotal roles in carcinogenesis and survival of cancer cells. Int J Mol Sci. 2014;15:12543–57. [PubMed: 25029543]

[50]. Pursell ZF, McDonald JT, Mathews CK, Kunkel TA. Trace amounts of 8-oxo-dGTP in mitochondrial dNTP pools reduce DNA polymerase gamma replication fidelity. Nucleic Acids Res. 2008;36:2174–81. [PubMed: 18276636]

[51]. Randerath K, Zhou GD, Somers RL, Robbins JH, Brooks PJ. A 32P-postlabeling assay for the oxidative DNA lesion 8,5'-cyclo-2'-deoxyadenosine in mammalian tissues: evidence that four type II I-compounds are dinucleotides containing the lesion in the 3' nucleotide. J Biol Chem. 2001;276:36051–7. [PubMed: 11454870]

[52]. Miller H, Prasad R, Wilson SH, Johnson F, Grollman AP. 8-oxodGTP incorporation by DNA polymerase beta is modified by active-site residue Asn279. Biochemistry. 2000;39:1029–33. [PubMed: 10653647]

[53]. Boguszewska K, Szewczuk M, Kazmierczak-Baranska J, Karwowski BT. How (5'S) and (5'R) 5',8-Cyclo-2'-Deoxypurines Affect Base Excision Repair of Clustered DNA Damage in Nuclear Extracts of xrs5 Cells? A Biochemical Study. Cells. 2021;10.

[54]. Nyaga SG, Jaruga P, Lohani A, Dizdaroglu M, Evans MK. Accumulation of oxidatively induced DNA damage in human breast cancer cell lines following treatment with hydrogen peroxide. Cell Cycle. 2007;6:1472–8. [PubMed: 17568196]

[55]. Szatrowski TP, Nathan CF. Production of large amounts of hydrogen peroxide by human tumor cells. Cancer Res. 1991;51:794–8. [PubMed: 1846317]

[56]. Birincioglu M, Jaruga P, Chowdhury G, Rodriguez H, Dizdaroglu M, Gates KS. DNA base damage by the antitumor agent 3-amino-1,2,4-benzotriazine 1,4-dioxide (tirapazamine). J Am Chem Soc. 2003;125:11607–15. [PubMed: 13129365]

[57. Gandhi V, Mineishi S, Huang P, Chapman AJ, Yang Y, Chen F, et al. Cytotoxicity, metabolism, and mechanisms of action of 2',2'-difluorodeoxyguanosine in Chinese hamster ovary cells. Cancer Res. 1995;55:1517–24. [PubMed: 7533664]

[58]. Prakasha Gowda AS, et al. Incorporation of gemcitabine and cytarabine into DNA by DNA polymerase beta and ligase III/XRCC1. Biochemistry 2010;49(23):p. 4833–40. [PubMed: 20459144]

[59]. Saif MW, Syrigos KN, Katirtzoglou NA. S-1: a promising new oral fluoropyrimidine derivative. Expert Opin Investig Drugs. 2009;18:335–48.

Highlights

- DNA repair polymerase can incorporate and misincorporate cdA lesions.
- The incorporated cdA can be readily extended and ligated into duplex DNA.
- The incorporation of cdA is mediated by nucleophilic attack without hydrogen bond.

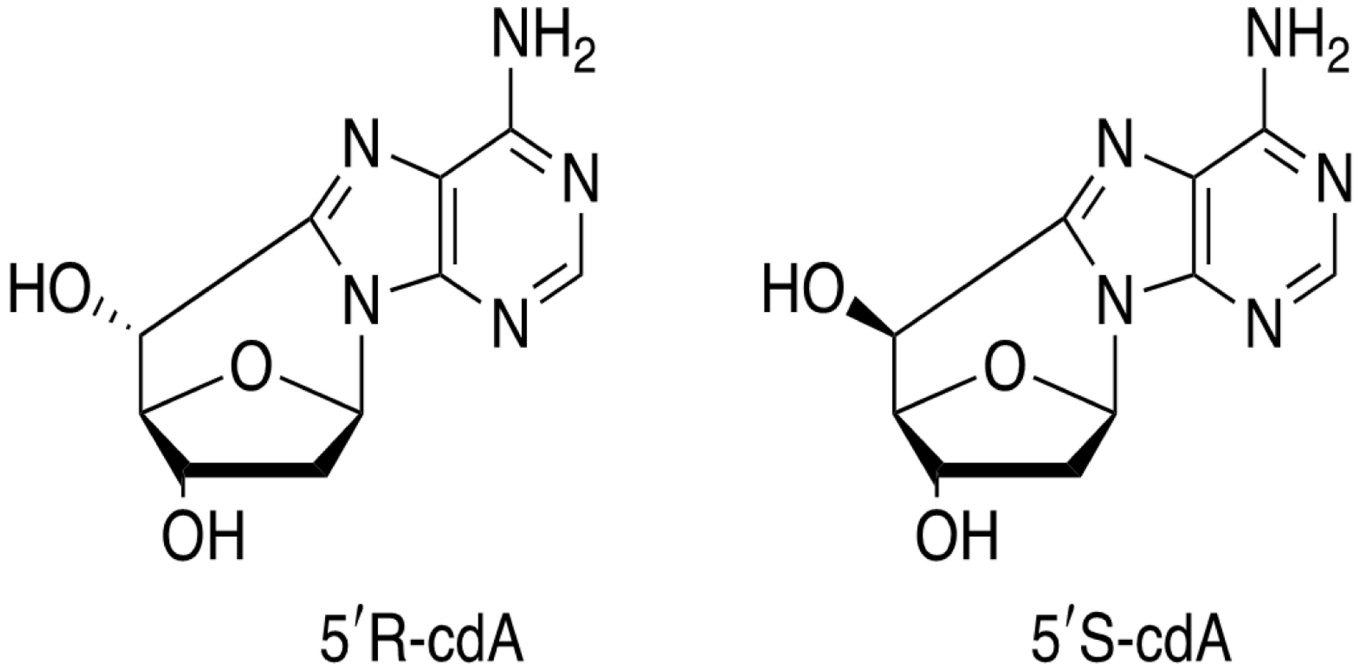

Figure 1. The structure of 5', 8-cyclo-2'-deoxyadenosine in 5'R and 5'S diastereoisomeric forms

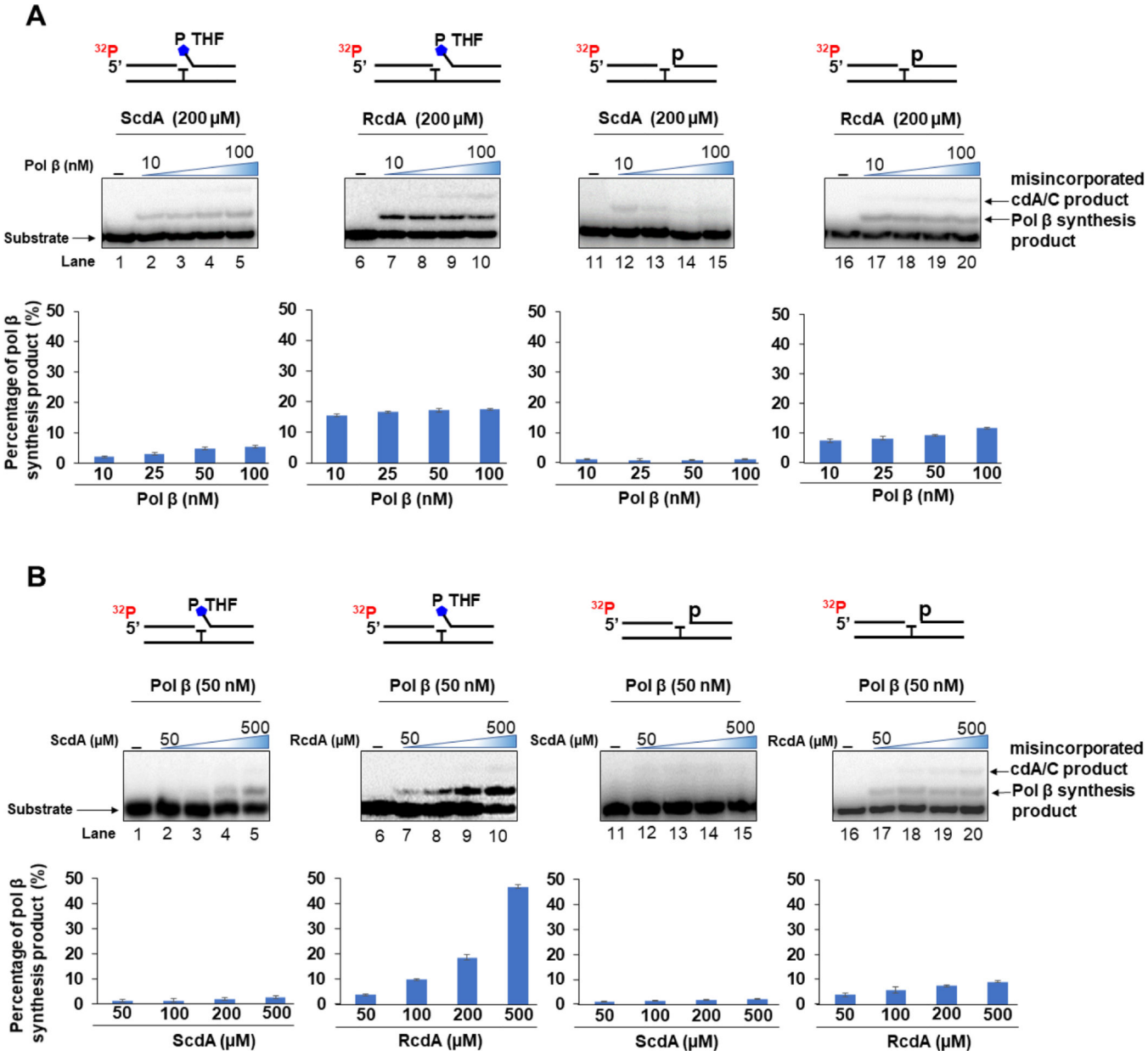

Figure 2. The incorporation of cdA by pol β during BER.

(A) The incorporation of cdA by pol β was determined in the presence of increasing concentrations of pol β (10, 25, 50, and 100 nM). Lanes 2–6 show the incorporation of 5'S-cdA by pol β 1 nt-gap substrate containing a tetrahydrofuran (THF) residue in the downstream primer. Lanes 8–12 illustrate the incorporation of 5'R-cdA by pol β with the substrate containing a THF residue at the downstream strand. Lanes 14–18 represent the incorporation of 5'S-cdA by pol β with the substrate having a phosphate at the 5'-end of the downstream primer. Lanes 20–24 indicate the incorporation of 5'R-cdA by pol β with the substrate containing a phosphate at the 5'-end of the downstream primer. (B) The incorporation of cdA by pol β in the presence of increasing concentrations of cdA (50, 100, 200, and 500 μM). Lanes 2–6 represent the incorporation of 5'S-cdA by pol β with

the 1 nt-gap substrate containing a THF residue in the downstream primer. Lanes 8–12 indicate the incorporation of 5’R-cdA by pol β with the substrate having a THF residue in the downstream primer. Lanes 14–18 illustrate the incorporation of 5’R-cdA by pol β with the substrate containing a phosphate at the 5’-end of the downstream primer. Lanes 20–24 represents the incorporation of 5’R-cdA by pol β with the substrate containing a phosphate at the 5’-end of the downstream primer. Lane 1, 7, 13, and 19 represents substrate alone. All experiments were done at least in triplicate. The quantification of the results is shown below the gels. The percentage of the products is illustrated as average ± SD in the bar charts.

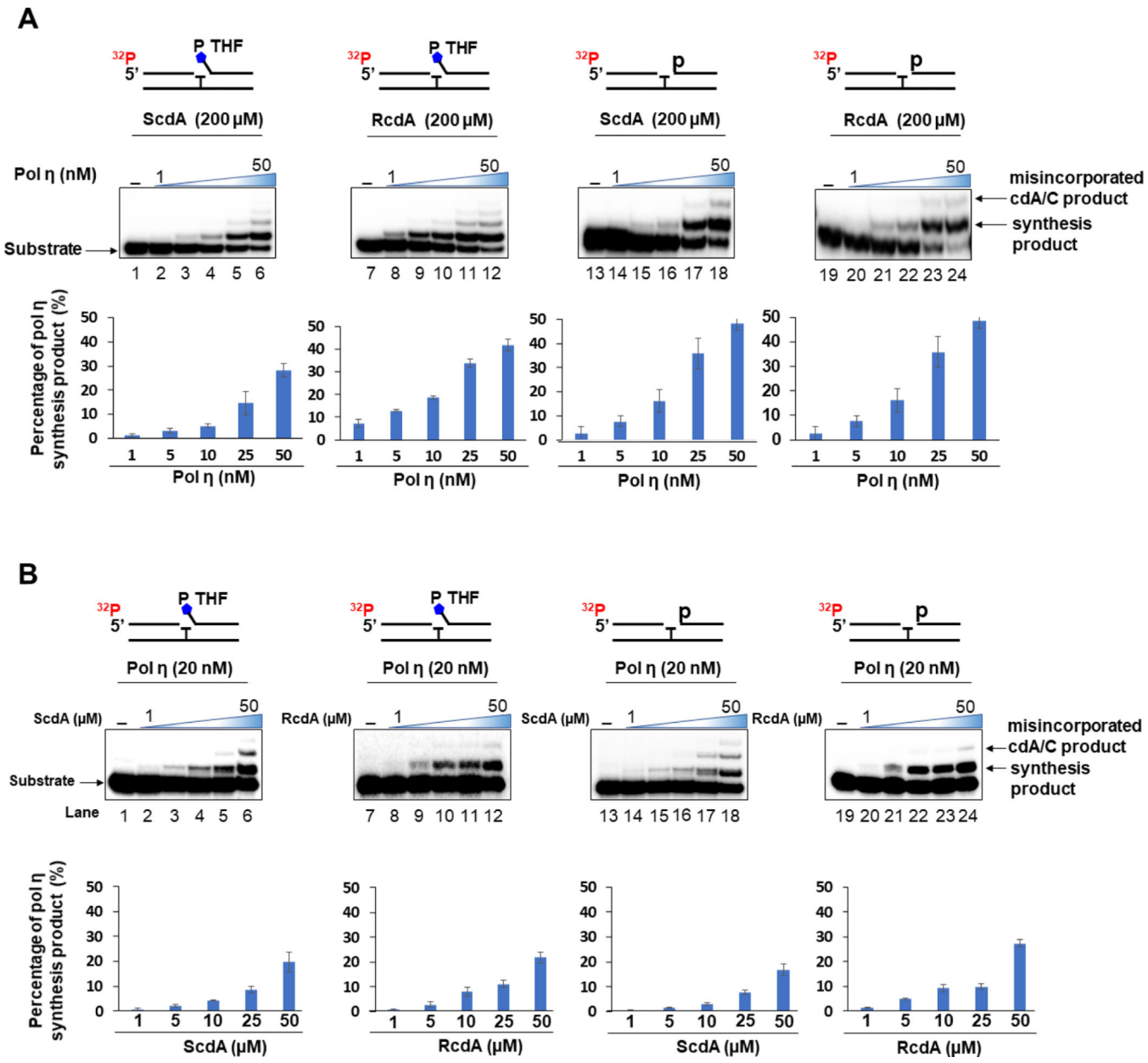

Figure 3. The incorporation of cdA by pol η during BER.

(A) The incorporation of cdA by pol η was determined in the presence of cdA (200 μM) and increasing concentrations of pol η (1, 5, 10, 25, and 50 nM). Lanes 2–6 illustrate the incorporation of 5'S-cdA by pol η with the 1 nt-gap substrate containing a THF in the downstream primer. Lanes 8–12 represent the incorporation of 5'R-cdA by pol η with the substrate containing a THF in the downstream primer. Lanes 14–18 indicate the incorporation of 5'S-cdA by pol η with the substrate containing a phosphate at the 5'-end of the downstream primer. Lanes 20–24 represent the incorporation of 5'R-cdA by pol η with the substrate containing a phosphate at the 5'-end of the downstream primer. (B) The incorporation of cdA by pol η (20 nM) in the presence of increasing concentrations of cdA (1, 5, 10, 25, and 50 μM). Lanes 2–6 represent the incorporation of 5'S-cdA by

pol η with the substrate containing a THF residue in the downstream primer. Lanes 8–12 illustrate the incorporation of 5'RcdA by pol η with the substrate containing a THF residue in the downstream primer. Lanes 14–18 indicate the incorporation of 5'S-cdA by pol η with the substrate containing a phosphate at the 5'-end of the downstream primer. Lanes 20–24 represent the incorporation of 5'R-cdA by pol η with the substrate containing a phosphate at the 5'-end of the downstream primer. Lane 1, 7, 13, and 19 represents substrate alone. All experiments were performed at least in triplicate. The quantification of the results is illustrated below the gels. The percentage of the products is illustrated as average ± SD in the bar charts.

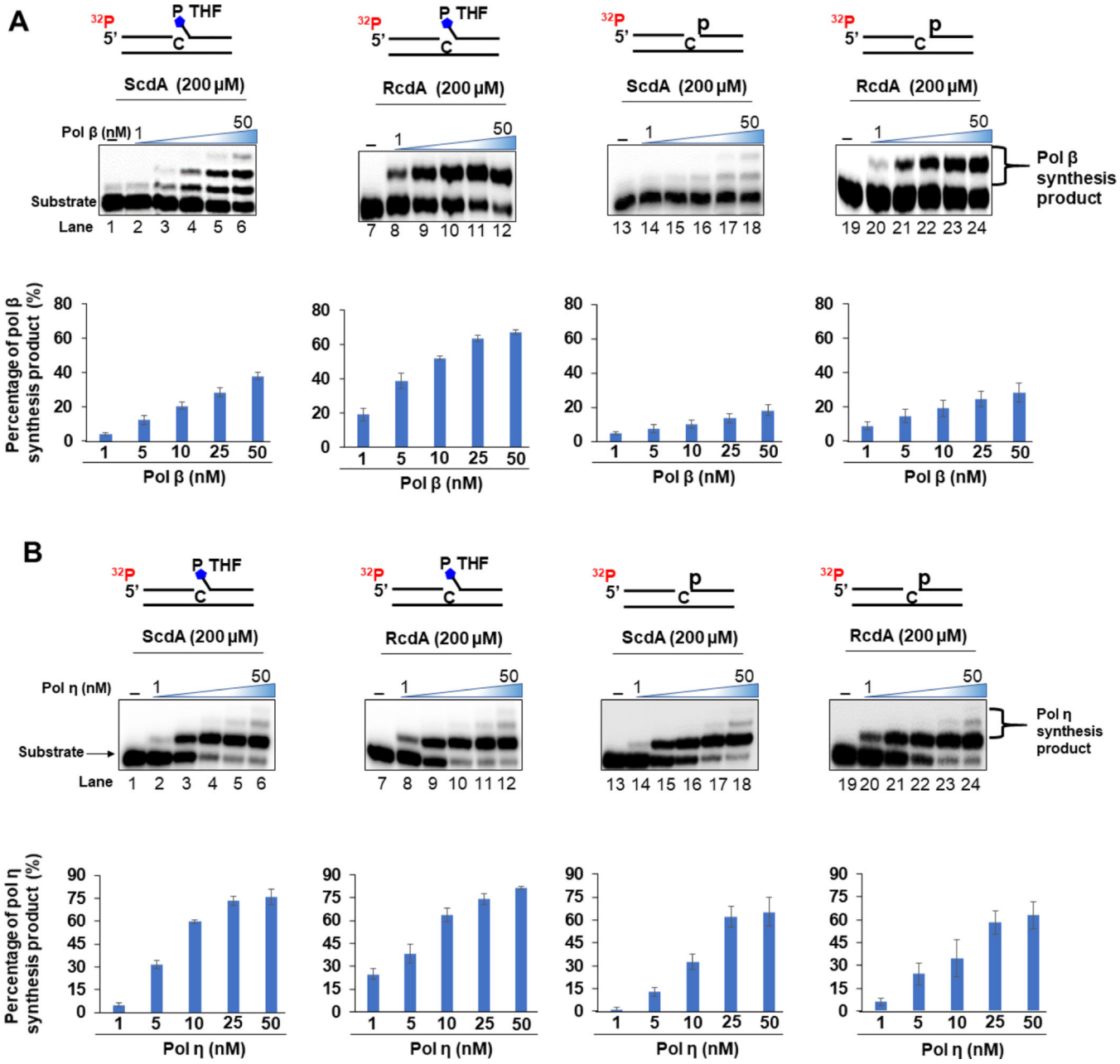

Figure 4. The misincorporation of cdA with a dC by pol β and pol η during BER.

(A) The misincorporation of cdA by pol β in the presence of a fixed concentration of cdA (200 μM) and increasing concentrations of pol β (1, 5, 10, 25, and 50 nM). Lanes 2–6 represent the misincorporation of 5'S-cdA by pol β with the 1 nt-gap substrate containing a THF residue at the downstream primer. Lanes 8–12 illustrate the misincorporation of 5'R-cdA by pol β with the substrate containing a THF in the downstream primer. Lanes 14–18 represent the misincorporation of 5'S-cdA by pol β with the substrate containing a phosphate at the 5'-end of the downstream primer. Lanes 20–24 indicate the misincorporation of 5'R-cdA by pol β with the substrate containing a phosphate at the 5'-end of the downstream primer. (B) The misincorporation of cdA by pol η was determined

in the presence of a fixed concentration of cdA (200 μM) and titrated concentration of pol η (1, 5, 10, 25, 50 nM). Lanes 2–6 represent the misincorporation of 5'S-cdA by pol η with the substrate containing a THF residue in the downstream primer. Lanes 8–12 illustrate the misincorporation of 5'RcdA by pol η with the substrate containing a THF residue in the downstream primer. Lanes 14–18 indicate the misincorporation of 5'R-cdA by pol η with the substrate containing a phosphate at the 5'-end of the downstream primer. Lanes 20–24 illustrate the misincorporation of 5'S-cdA by pol η with the substrate containing a downstream 5'-phosphate. Lane 1, 7, 13, and 19 represents substrate alone. All experiments were performed at least in triplicate. The quantification of the results is illustrated below the gels. The percentage of the products is illustrated as average ± SD in the bar charts.

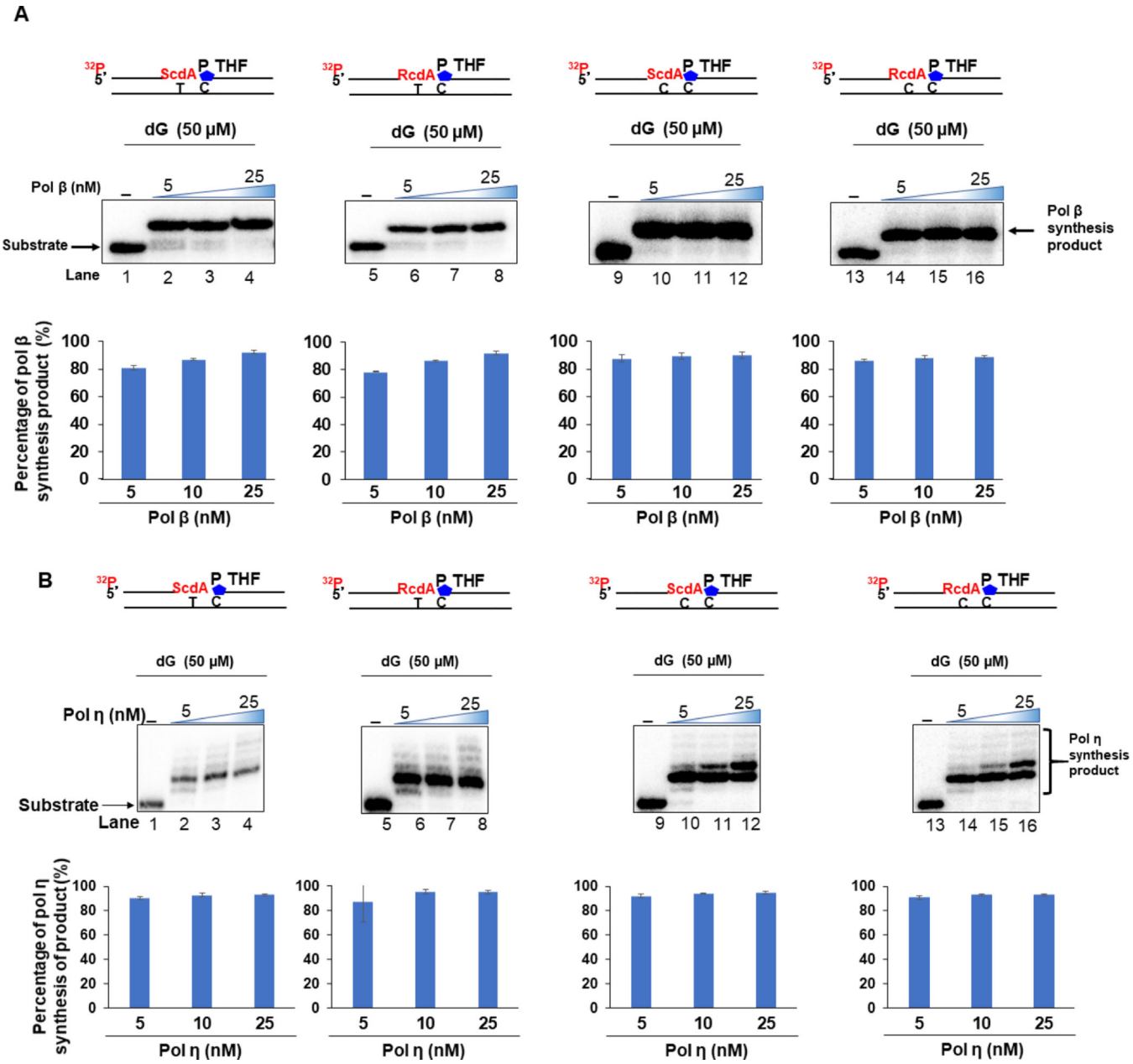

Figure 5. Extension of cdA base paired with dT or dC by pol β and pol η.

(A) The extension of cdA by pol β was determined in the presence of a fixed concentration of dG (50 μM) and increasing concentrations of pol β (5, 10, and 25 nM). Lanes 2–4 represent the extension of 5'S-cdA basepaired with dT by pol β with the 1 nt-gap substrate containing a THF residue at the downstream primer. Lanes 6–8 illustrate the extension of 5'R-cdA basepaired with dT by pol β with the substrate containing a downstream 5'-THF residue. Lanes 10–12 represent the extension of 5'S-cdA basepaired with dC by pol β with substrate containing a downstream 5'THF residue. Lanes 14–16 indicate the extension of 5'R-cdA basepaired with dC by pol β with the substrate containing a downstream 5'-THF residue. (B) The extension of cdA by pol η was determined in the presence of a fixed concentration of dG (50 μM) and increasing concentrations of pol η (5, 10, and 25 nM).

Lanes 2–4 represent the extension of 5’S-cdA basepaired with dT by pol η with the 1 nt-gap substrate containing a 5’-THF residue. Lanes 6–8 illustrate the extension of the 5’R-cdA basepaired with dT by pol η with the THF-containing substrate. Lanes 10–12 represent the extension of the 5’S-cdA basepaired with dC by pol η with the THF-containing substrate. Lanes 14–16 indicate the extension of the 5’R-cdA base paired with dC by pol η with the THF-containing substrate. Lane 1, 5, 9, and 13 represents substrate alone. All experiments were performed at least in triplicate. The quantification of the results is illustrated below the gels. The percentage of the products is illustrated as average ± SD in the bar charts.

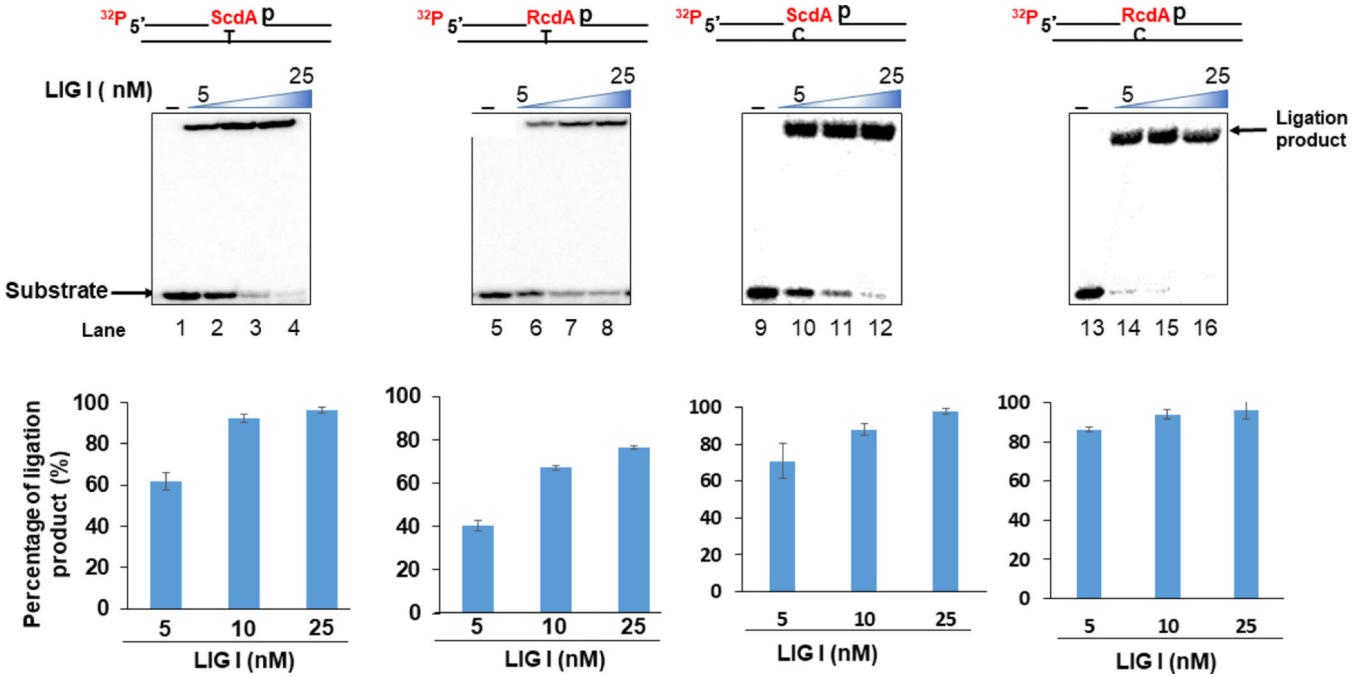

Figure 6. Ligation of cdA by DNA LIG I.

Ligation of cdA basepaired with dT or dC by LIG I. The ligation of cdA by LIG I was measured in the presence of increasing concentrations of LIG I (5, 10, and 25 nM). Lanes 2–4 represent the ligation of 5'S-cdA basepaired with dT with the nicked substrate containing a 5'-phosphate at the downstream primer. Lanes 6–8 illustrate the ligation of 5'R-cdA basepaired with dT with the nicked substrate. Lanes 10–12 represent the ligation of 5'S-cdA basepaired with dC with the nicked substrate. Lanes 14–16 indicate the ligation of 5'R-cdA basepaired with the nicked substrate. Lane 1, 5, 9, and 13 represents substrate alone. All experiments were performed at least in triplicate. The quantification of the results is illustrated below the gels. The percentage of the products is illustrated as average ± SD in the bar charts.

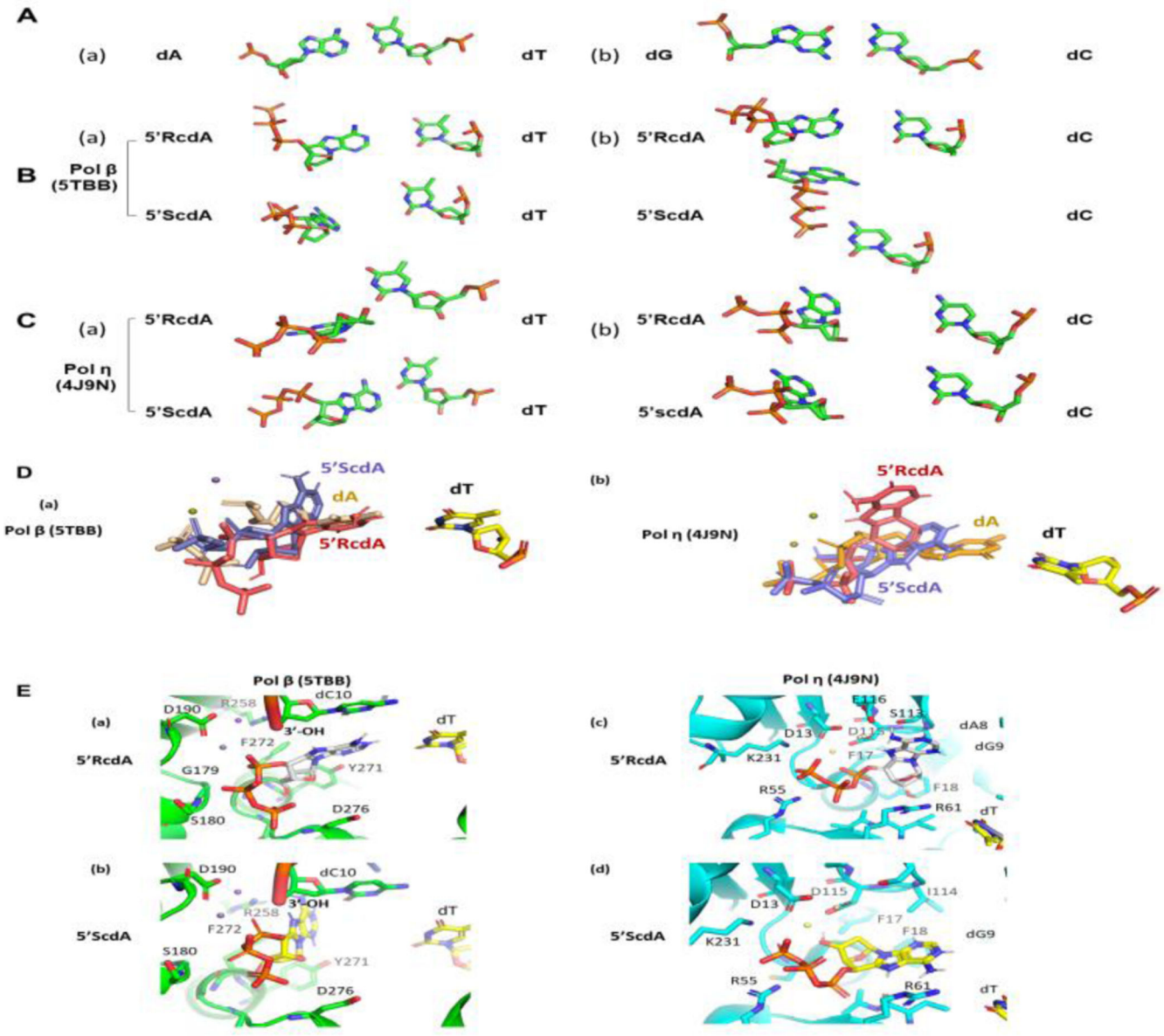

Figure 7. The molecular docking analysis on the interaction between pol β and pol η and cdA.

(A) (a) The docked structure of dA:dT basepair. (b) The docked structure of dG against dC. (B) (a) The docked structure of pol β with 5'R- or 5'S-cdA opposite a template dT. (b) The docked structure of pol β with 5'R- and 5'S-cdA opposite a template dC. (C) (a) The docked structure of pol η with 5'R- and 5'S-cdA opposite a template dT. (b) The docked structure of pol η with 5'R- and 5'S-cdA opposite a template dC. (D) (a) The superimposed docking structure of pol β with dA, 5'R-cdA, and 5'S-cdA opposite dT. (b) The superimposed docking structure of pol η with dA, 5'R-cdA, and 5'S-cdA opposite dT. (E) (a) The amino acids surrounding 5'R-cdA opposite to dT in the active site of pol β. (b) The amino acids that were around 5'ScdA opposite to dT in the active site of pol β. (c) The amino acids that were around 5'R-cdA opposite dT in the active site of pol η. (d) The amino acids that are around 5'S-cdA opposite dT in the active site of pol η.

Table I

Steady state kinetics of the incorporation and extension of cdA by Pol β

Substrate	*Km,cdA* (μM)	*kcat,cdA* (10–4 s-1)	$k_{cat,cdA}/K_{m,cdA}$ (10–6 μM-1 s-1)	*Km,DNA* (10–2 μM)	*kcat,DNA* (10–4 s-1)	$k_{cat,DNA}/K_{m,DNA}$ (10–2 μM-1 s-1)
RcdA : dT	122 ± 64	8.20	6.70	3.52 ± 0.70	7.03 ± 0.67	2.00
RcdA : dT (THF)	141 ± 53	18.50	13.10	7.96 ± 1.60	23.39 ± 1.50	2.94
ScdA : dT	ND	ND	ND	ND	ND	ND
ScdA : dT (THF)	ND	ND	ND	ND	ND	ND
RcdA : dC	193 ± 52	12.00	6.20	1.91 ± 0.72	6.50 ± 1.03	3.40
RcdA : dC (THF)	355 ± 99	22.00	6.20	2.97 ± 0.61	14.01 ± 2.32	4.71
ScdA : dC	241 ± 14	10.00	4.20	5.83 ± 1.40	18.83 ± 3.30	3.23
ScdA : dC (THF)	398 ± 143	16.10	4.10	1.21 ± 0.49	8.03 ± 2.10	6.64
RcdA : dT extension	20.50 ± 1.87	14.74	71.70	0.81 ± 0.17	2.25 ± 0.45	2.78
ScdA : dT extension	30.25 ± 4.13	35.50	117.36	4.17 ± 2.40	7.73 ± 1.77	1.85
RcdA : dC extension	44.1 ± 5.00	8.72	19.77	2.02 ± 0.59	39.10 ± 6.73	19.40
ScdA : dC extension	56.0 ± 15.6	10.40	18.57	3.67 ± 0.96	57.10 ± 8.88	15.60

THF: a tetrahydrofuran residue with a phosphate group at the 5’-end of the downstream primer of the substrates

ND: Measurable enzyme kinetic parameters were not able to be obtained due to the extremely low percentage of 5’S-cdA incorporation products.

The results represent average ± SD and were obtained from at least three independent experiments.

Table II

Steady state kinetics of the incorporation and extension of cdA by Pol η

Substrate	*Km,cdA* (μM)	*kcat,cdA* (10–4 s-1)	$k_{cat,cdA}/K_{m,cdA}$ (10–5 μM-1 s-1)	*Km,DNA* (10–2 μM)	*kcat,DNA* (10–4 s-1)	$k_{cat,DNA}/K_{m,DNA}$ (10–2 μM-1 s-1)
RcdA : dT	157.5 ± 15.9	38.40	2.44	1.32 ± 0.21	10.33 ± 0.85	7.83
ScdA : dT	62.47 ± 12.0	25.80	4.13	2.16 ± 1.12	9.63 ± 0.63	4.46
RcdA : dC	222 ± 23.4	155	6.98	1.82 ± 0.33	17.64 ± 2.12	9.69
ScdA : dC	91.04 ± 29.7	114	12.52	4.39 ± 0.08	30.53 ± 1.87	6.95
RcdA : dT extension	2.83 ± 1.27	31.1	109.89	1.21 ± 0.01	197.30 ± 10.60	163.10
ScdA : dT extension	3.06 ± 1.69	18.63	60.8	1.00 ± 0.36	158.60 ± 12.70	158.60
RcdA : dC extension	7.37 ± 2.35	25.00	33.9	12.50 ± 1.93	1622.30 ± 275.10	129.78
ScdA : dC extension	4.02 ± 0.85	15.15	37.7	6.83 ± 1.01	884.80 ± 182.00	129.55

The results represent average ± SD and were obtained from at least three independent experiments.